JOURNAL OF APPLIED ELECTROCHEMISTRY 26 (1996) 18–29

Electrochemical treatment of human wastes in a packed bed reactor

C. L. K. TENNAKOON*, R. C. BHARDWAJ‡, J. O'M. BOCKRIS

Surface Electrochemistry Laboratory, Texas A&M University, College Station, TX 77843-3255

Received 31 May 1994; revised 10 April 1995

There is an increasing interest in the use of electrochemical methods for dealing with pollution problems. This paper deals with the mass balance and the use of a packed bed reactor for the electrochemical incineration of human wastes. Parametric studies were carried out to determine the effect of: (i) anodic particle size, (ii) flow rate of faeces/urine mixture, (iii) height of packed bed, (iv) current density and (v) cathode to anode spacing arrangement, on the rate of oxidation of human waste. It is shown that particles of Ebonex^{TM} (0.5–1.0 mm diam.) coated with a catalyst layer, comprising SnO_2/Sb_2O_3, a solution flow rate of 0.9–1.4 cm s^{-1} through the packed bed based on the cross sectional area of the reactor, a bed height of 5–8 cm and a current density based on the geometric area of the particles of 5 mA cm^{-2} comprise an optimum set of parameters for the scale-up of a packed-bed electrochemical reactor system. A preliminary design for the further scale up of the process is also described.

1. Introduction

There is growing concern regarding the disposal of human wastes. Presently, sewage treatment work in urban areas at central locations is becoming less efficient as the throughput of wastes in these plants is increasing [1]. Thus, small waste disposal units in each household are an attractive alternative. If electrochemical oxidation of wastes is the preferred path, such units might even be powered by roof situated solar panels.

There is also increasing concern regarding the disposal of human wastes in space missions of long duration. It will be necessary to convert such wastes into products which can be recycled into an environmental control and life support system (ECLSS) [2], which incorporates the growth of plants (e.g., wheat) and algae to provide sustenance for astronauts. Chemical treatments have proven relatively unsatisfactory, more so with increase in the mission duration. Thermal conversion of wastes to CO_2 involves dissipating heat in a space environment and the generation of byproducts containing nitrogen oxides and carbon monoxide in the effluent gases [3, 4]. Electrochemical techniques offer several advantages including low temperatures and the absence of NO_x and CO in the evolved gases.

Investigations into the electrochemical oxidation of human wastes have been conducted for several years in this laboratory. In the pioneering work of Bockris *et al.* [5], it was shown that cellulose could be broken down to CO_2 with a current efficiency of nearly 100% and that only two faradays of electricity were involved in the evolution of 1 mol of CO_2 perhaps because of the preliminary acid hydrolysis of cellulose to glucose.

Other contributions in the electrochemical oxidation of wastes include the work by Dhooge [6] in which conversion of cattle manure and wood chips into pollution free products containing no CO or oxides of nitrogen was described. In this study various redox couples, for example, iron (II)/iron (III), cobalt (II)/cobalt (III), vanadium (IV)/vanadium (V) were used. Electrochemical oxidation of urea in urine was reported by Tischer *et al.* [7].

A systematic study of the oxidation of human wastes commenced with a fundamental investigation into their composition and the oxidizability of the components by electrochemical means. In this initial study Kaba, Hitchens and Bockris [8, 9] showed that an artificial waste mixture could be prepared having a similar composition to that of human faeces: cellulose, oleic acid, casein and microbial biomass consisting of *Torpulina*. It was found that these could all be disposed of by an electrochemical process involving a platinum electrode in 5–12 M sulfuric acid at temperatures up to 150 °C. The use of the Ce^{3+}/Ce^{4+} redox couple was also studied. An increase in the oxidation rate of about 40% was reported in the presence of the redox couple compared to that in its absence [9].

At this stage (1990), it was decided to exclude the use of H_2SO_4 and to carry out the oxidation of faeces–urine mixture at temperatures less than 100 °C. When this mixture was electrolysed, at about 90 °C, 95% consumption of the faeces–urine content was obtained in about the same time as that used for the consumption of the waste mixture in concentrated sulfuric acid at 150 °C. This increase in rate

* Present address: Lynntech, Inc., 7610 Eastmark Drive, College Station, TX 77840.
‡ Present Address: Lockheed Engineering and Sciences Company, White Sands Facility, Las Cruces, NM 88004.

0021-891X/93

was explained as due to the action of HOCl, which is formed by the partial hydrolysis of small amounts of chlorine formed at the anode [9], by the oxidation of chloride ions in urine. Additional sodium chloride was not added to the waste mixture.

The next phase was to look for a suitable electrode material for the oxidation of the faeces–urine mixture [10]. Seven different electrocatalysts, namely, Pt, PbO_2, Au, graphite, perovskite ($La_{0.79}Sr_{0.21}MnO_3$), tungsten carbide and Ebonex^{TM} material coated with RuO_2 had been used. It was found that perovskite and RuO_2 coated Ebonex^{TM} were superior to other electrodes investigated because of their enhanced catalytic activity and mechanical stability. These studies were performed in glass 'U' type cells.

This study reports the following two aspects of the electrochemical oxidation of wastes which have not been considered earlier: (i) Mass balance study of the electrochemical oxidation process in a 'U' tube cell. (ii) The scaling up of the process by using parallel plate electrodes with high solution flow rates and a packed bed electrode with a high surface area-to-volume ratio.

2. Experimental details

2.1. *Studies in 'U' tube cells*

A simple glass U-tube cell was utilized. The cathode and anode compartments were not separated. The anode compartment was provided with a calomel reference electrode and a Luggin capillary to make measurements of anode potential with a minimum *IR* component. A magnetic stirrer was used to stir the waste mixture during the experiments.

The cathode was a platinum gauze about 4 cm × 3 cm. The anode was a cylindrically shaped platinum electrode 5 cm long and about 3.5 cm in diameter, that is, with both sides a working area of about 100 cm^2.

Constant potential experiments were conducted at 1.44, 1.74, 1.90 and 2.00 V on the normal hydrogen scale and the temperature of electrolysis was 90 °C. The potentials were corrected for *IR* drop between the Luggin capillary and the working electrode using an Electrosynthesis 800 *IR* measurement system.

In the constant current work the current density was 7.5, 8, 10 and 12 mA cm^{-2} in successive runs.

A Pine potentiostat (RDE4) was used and the total quantity of electricity passed was measured using a Electrosynthesis 640 digital coulometer. The coulometer was used because the current varied with time during potentiostatic runs.

2.2. *Studies with parallel plate cell*

The first attempt on the scaling up of the process used a parallel plate electrochemical cell (Electrocell AB). This cell was constructed in a similar manner to a plate and frame filter press which consisted of a cathode, an anode, a separator and plastic frames through which the electrolyte was introduced into and removed from the cell. The cell had an effective area of 100 cm^2 and an interelectrode gap of 0.5 cm. A maximum electrolyte flow rate of about 500 litres per hour could be established through the inter-electrode gap. The two electrodes were separated by a 'Celgard' membrane. Turbulence promoting nets provided by the manufacturer were used in both anodic and cathodic compartments. Anodes used were graphite, lead dioxide and ruthenium dioxide coated titanium. The cathode was a stainless steel plate. This cell was used to obtain polarization curves for the electrochemical oxidation of the waste mixture at 90 °C as a function of flow rate of the waste solution.

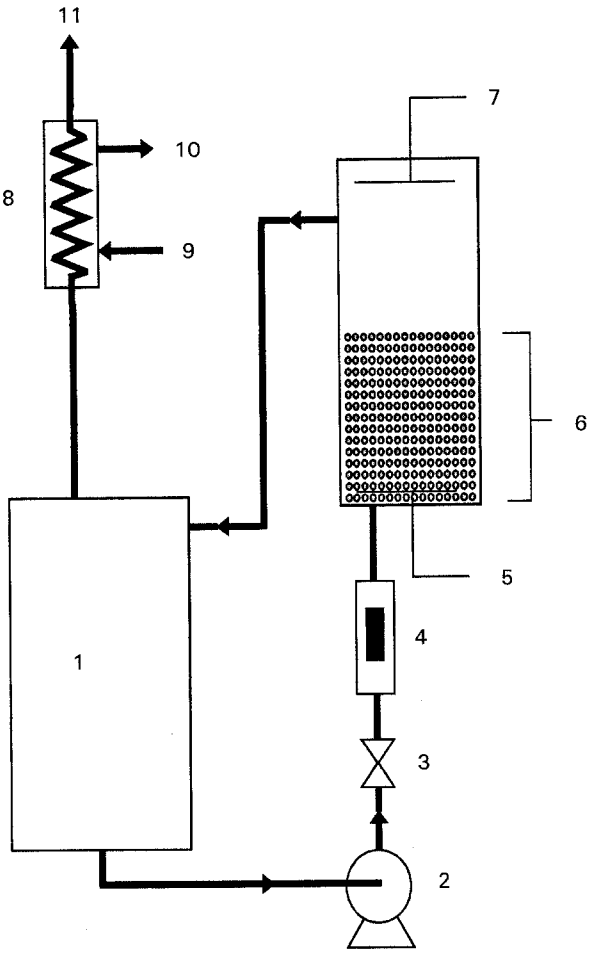

Fig. 1. Schematic diagram of the packed bed cell and the flow circuit. (1) Reservoir, (2) pump, (3) valve, (4) flow meter, (5) anode current collector, (6) packed bed anode, (7) cathode, (8) water condenser, (9) water inlet, (10) water outlet and (11) outlet for gases.

2.3. *Studies with packed bed reactors*

Figure 1 shows a schematic diagram of a packed bed cell and the associated flow circuit. A glass tube of 3 cm internal diameter fitted with a glass frit served as the support for the Ebonex^{TM} or graphite particles forming the bed. The height from the bottom of the bed to the flow exit was 13.5 cm. Particles of several different sizes were used in the experiments detailed in the succeeding sections. Similarly,

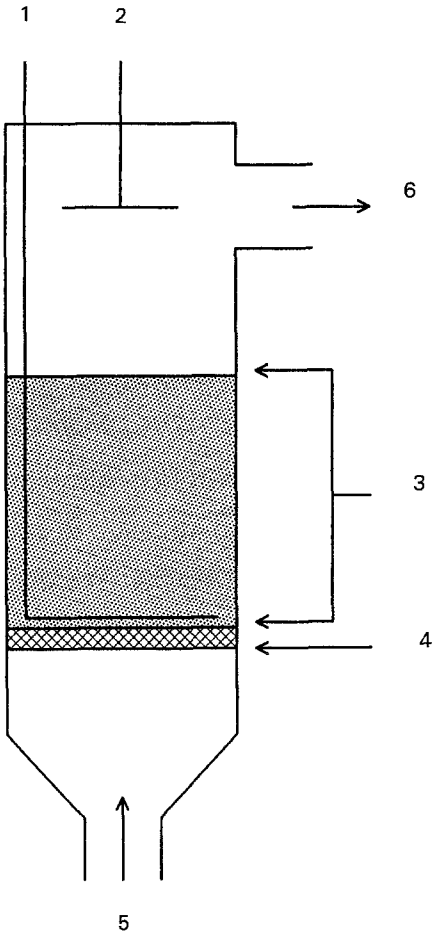

Fig. 2. Packed bed cell with solution flow parallel to current lines. (1) Anode current collector, (2) cathode, (3) packed bed anode, (4) bed support, (5) flow inlet and (6) flow outlet.

different configurations of the packed bed were used in the experiments.

2.3.1. Current lines in the direction of waste solution flow. In this configuration the feeder (anode current collector) electrode was placed at the bottom of the bed, which was a platinum mesh of area 7 cm^2. The electrical connection was made to this feeder electrode through a lead sealed inside a glass tube, positioned vertically from the top of the cell.

The counter electrode was a stainless steel sheet of 7 cm^2 positioned above the bed of particles. A membrane separating the anode and cathode was not used when using this configuration shown in Fig. 2.

2.3.2. Current lines in the direction perpendicular to the solution flow. Several alternative configurations were used in the experiments, the first being shown in Fig. 3. In this configuration the feeder (anode current collector) was a platinum mesh formed into a cylinder of internal diameter 2 cm. The cathode consisted of three titanium rods each of 3.175 mm in diameter, electrically connected together and placed centrally in the bed. The three cathode stanchions were insulated from the anode bed of particles by surrounding them with a proton exchange Nafion® membrane formed into a cylindrical shape as shown in Fig. 3. The same waste solution was in contact

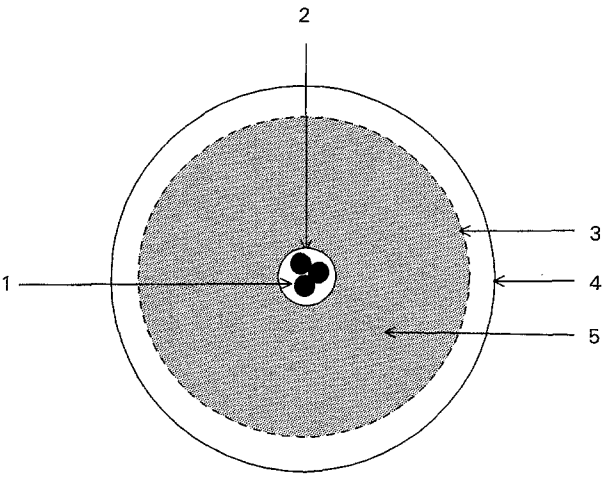

Fig. 3. Cross section of packed bed cell with a central cathode. (1) Cathode consisting of three titanium rods 3.175 mm diam., (2) Nafion® membrane, (3) platinum mesh anode current collector, (4) glass cell and (5) packed bed.

with the anode bed and cathode stanchions. The cell was filled with Ebonex™ particles coated with SnO_2 doped with Sb_2O_3 to the required height. The particles resting within the current collector and central cathode were effectively participating in the reaction. The advantage of this configuration is the reduced distance between anode and cathode, thereby lowering the operating voltage. This configuration was particularly necessary to study the performance of the packed bed as a function of bed height.

A further refinement of this design is shown in Fig. 4. Here five cathode stanchions are arranged within the bed, thus decreasing the cathode to anode current collector distance. A still further refinement is shown in Fig. 5. In this design the anode current collectors consisted of the cylindrical mesh, as well as a central anode stanchion. Here the four cathodes (Ti rods marked 1, 2, 3 and 4) were situated between the two anode current collectors, the mesh and the central stanchion marked 5 in Fig. 5. The four cathodes were insulated from the anode by Nafion® membranes.

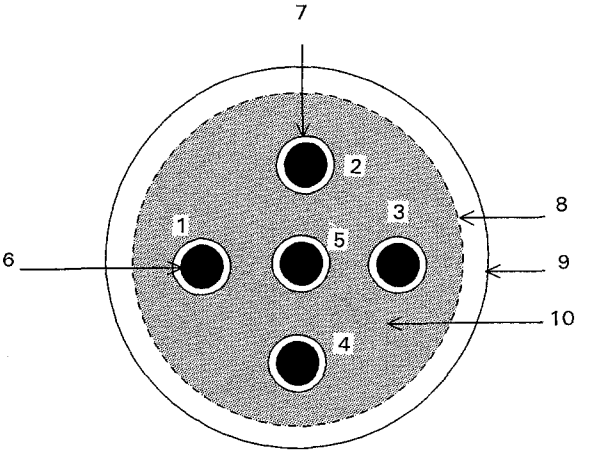

Fig. 4. Cross section of packed bed cell with five 3.175 mm diam. titanium cathode stanchions. (1, 2, 3, 4, 5) cathode stanchions surrounded by Nafion® membranes, (6) a cathode stanchion, (7) Nafion® membrane, (8) anode current collector, (9) glass cell and (10) packed bed.

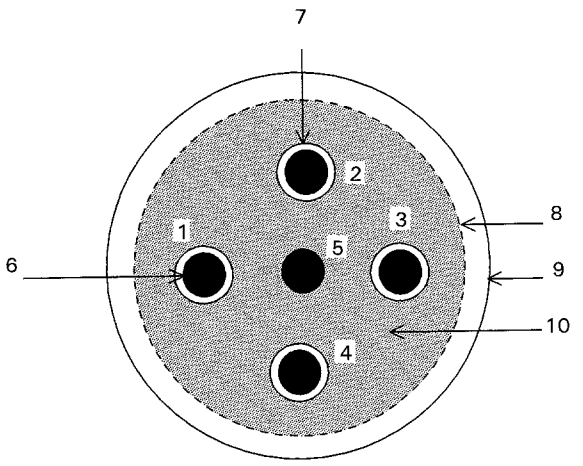

Fig. 5. Cross section of packed bed cell with four 3.175 mm diam. titanium cathode stanchions and a 3.175 diam. platinized titanium anode stanchion. (1, 2, 3, 4) Cathode stanchions surrounded by Nafion® membranes, (5) anode stanchion, (6) a cathode stanchion, (7) Nafion® membrane, (8) anode current collector, (9) glass cell and (10) packed bed.

During parametric studies, bed height was increased up to 10 cm and flow rate was increased up to 1250 mL min^{-1}.

2.3.3. Bed material. The first electrode material tested in the packed bed consisted of graphite particles with a mean diameter of 0.75 mm. It was observed that the electrochemical stability of these particles was poor; the particles slowly disintegrated with oxygen evolution. The next electrode material tested was 1 mm diameter Ebonex™ particles, coated with RuO_2 [10]. An 0.1 M solution of $RuCl_3$ in 50% aqueous propanol was prepared and the solution was evaporated to form a thick slurry. The particles were prepared by crushing a plate of Ebonex™ material and subsequent separation using standard sieves. The particles were then washed in distilled water, etched in 10% HF and dried at 120 °C. The coating slurry was then applied to the particles using a brush. Care was taken to ensure that all the particles were wet with the coating slurry. The solvent was allowed to evaporate at 110 °C and then the particles were placed in an oven at 400 °C for 5 min. The procedure was repeated four times and the final annealing was done at 400 °C for 1 h in the presence of air. Thereafter, the particles were cooled in air, washed in distilled water and stored.

The electrode material used in the majority of the experiments was Ebonex™ coated with SnO_2 doped with Sb_2O_3 using a slurry formulation modified from that used by Kotz, *et al.* [11], Stucki, *et al.* [12] and Comnisellis and Vercesi [13].

The solution used for coating the Ebonex™ material was 6.4 g $SnCl_2.2H_2O$, 0.1 g $SbCl_3$ in 100 ml of ethanol or propanol. Two methods of coating the particles were tried, namely (i) spray pyrolysis and (ii) brush painting. The solution for spray pyrolysis was made in ethanol, while the viscous slurry for brushing was made up in propanol.

Depth profile measurements using X-ray photoelectron spectroscopy (XPS) clearly showed that brush painting provided a thicker coating than spray pyrolysis.

The particles used in the experiments were prepared by the brush painting method described earlier for RuO_2 deposition except for the fact that the particles were initially degreased with 10% NaOH solution.

Table 1. Composition of the artificial faecal mixture

Component	*Total dry weight/%*
Cellulose	33
Torpulina	25
E. coli	07
Casein	10
Oleic acid	20
KCl	2
NaCl	2
$CaCl_2$	1

2.4. *Waste mixture*

A synthetic mixture of material which represented the main constituents of faeces was made up. Although the nature of sewage and faeces mixtures can vary considerably, generally one-third of its contents is made up of intestinal microorganisms and approximately one-third is made up of undigested fibre [14]. The remainder is made up of lipids and inorganic material. The waste mixture shown in Table 1 reflects these proportions. The microorganisms *Torpulina* and *E. coli* were obtained in powdered form from Sigma Chemical Company, and the remaining contents were obtained from standard chemical suppliers. All amounts of waste are given in terms of dry weight. A fresh batch of the waste mixture was prepared every month and the mixture was kept frozen between experiments.

Waste solutions were made up in urine without the addition of any supporting electrolytes. The solid material used for experiments consisted of 14 g waste (dry faeces) in a litre of urine. The material was weighed and treated in a pestle and mortar to which a small amount of urine was added. The mixture was then further homogenized for 4 h in a 600 watt sonicator (Fisher) working in a pulse mode with a duty cycle of 60%. The sonication was carried out in a special glass vessel. The essential feature of this vessel is that the lower part is conical so that the particles at the bottom are subjected to severe bombardment by the sonicator horn. Larger particles settle to the bottom and size reduction takes place as the process is repeated. During sonication the conical vessel was immersed in water at room temperature to prevent the waste solution from becoming unduly heated.

Samples of slurry subjected to sonication were placed on microscope slides and examined on a Nikon OPTIPHOT microscope using objective micrometres. This microscopic examination revealed that the particle size was about 25 μm.

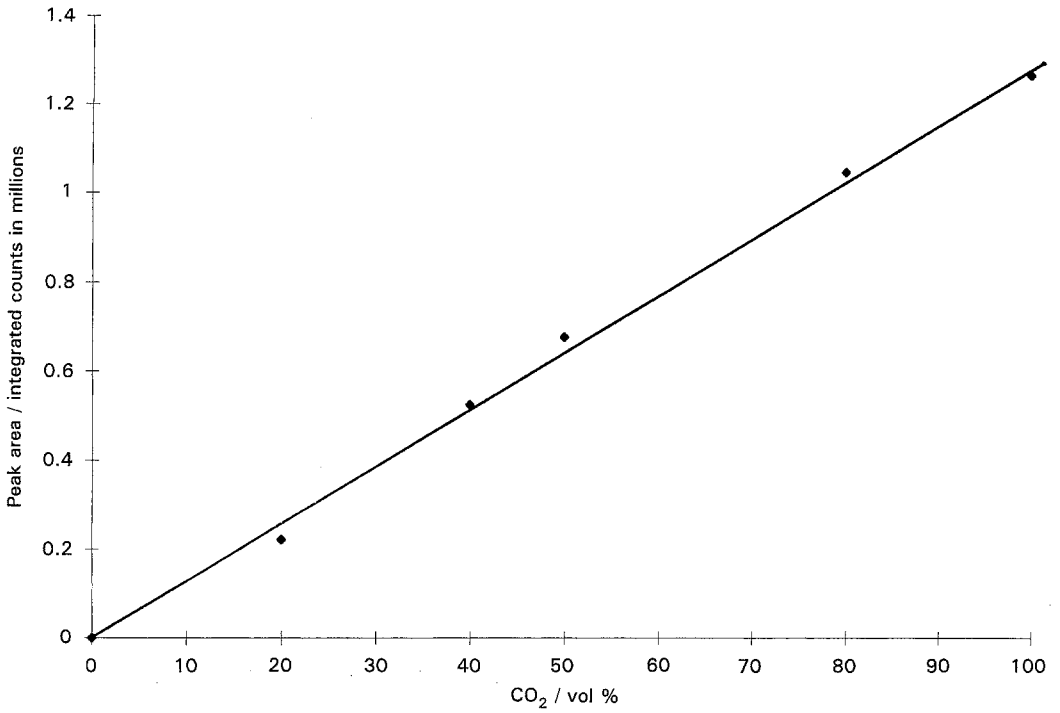

Fig. 6. Calibration graph for carbon dioxide gas.

2.5. *Collection of evolved gases*

The gases generated in the experiments using U-cells and the packed bed cells were passed through a water condenser (to condense back into the cell any water vapour and organics), two water traps to remove chlorine (to prevent damage to the gas chromatographic column) and were then collected by downward displacement of water (at 25 °C) in measuring flasks of 4 litre capacity. These flasks were emptied and refilled with water several times during electrolysis. Volumes of gases collected were noted before each refilling.

2.6. *Analytical techniques*

A Varian (model 3400) gas chromatograph with a Carbosieve SII column and a thermal conductivity detector were used for gas analysis. Argon was used as carrier gas at a flow rate of 30 mL min^{-1}. Chromatograms were recorded using a HP 3390 A Integrator which provided digital readouts of the retention times and integrated areas of the different peaks.

Calibration curves for H_2, O_2, N_2 and CO_2 were determined on a regular basis. A typical calibration curve for CO_2 is shown in Fig. 6, and similar curves with different slopes were obtained for other gases. Gas samples were taken at intervals of 4 to 5 h. The sample held 100 μL. The gas samples were injected into the gas chromatograph and by the characteristic peaks for nitrogen, hydrogen, CO_2 and oxygen, which had been previously calibrated, the percentages of different gases were calculated using the integrated areas recorded.

Details of analytical procedures for (a) the determination of chlorine by neutron activation analysis and (b) total organic carbon (TOC) measurement were given previously [8].

3. Results and discussion

3.1. *Constant current and constant potential experimental results*

Table 2 presents results for constant current conditions and Table 3 for constant potential conditions in U-cells. Comparing the results of Pt-15 and Pt8RR, it is seen that TOC reduction of 82% is achieved in 24.3 h at constant current, whereas in the constant potential experiment, TOC reduction of only 65% is achieved in 35.8 h. Thus, constant potential experiments yield slow overall reaction rates as the total current drops as the faecal matter becomes oxidized. On the other hand, constant current electrolysis yield higher rates of oxidation, presumably due to the following supportive oxidation processes:

(i) Generation of hypochlorous acid in the bulk phase which may be formed by hydrolysis of chlorine evolved during the oxidation of chloride ions in the waste mixture.

(ii) Generation of OH radicals, known as powerful oxidizing agents [15], according to

$$2H_2O \rightarrow 2OH^{\cdot}_{ads} + 2H^+ + 2e^-$$

(iii) Generation of OH radicals in the bulk solution by the decomposition of hydrogen peroxide which may be formed on the cathode by reduction of dissolved oxygen.

Table 2. Results of electrolysis of faecal–urine mixture at different current densities
Constant current electrolysis on platinum at 90 °C

Serial	*Applied current density* /mA cm^{-2}	*Charge* /C	*Electrolysis time* /h	*Initial dry mass of waste* /g		*Gases evolved* /mmol and (g)					*TOC initial* /mg L^{-1}	*TOC final* /mg L^{-1}	*Reduction in TOC* /%
				Faeces solids	*Urine solids*	CO_2	H_2	N_2	O_2	Cl_2			
Pt-1	7.5	848.3×10^2	31.4	1.86	3.36	48.8 (2.14)	396.7 (0.79)	31.7 (0.79)	40.0 (1.28)	0.97 (0.03)	5626	1528	72
Pt-5	8	1051×10^2	36.5	2.00	3.36	53.8 (2.36)	444 (0.88)	33.9 (0.95)	85.9 (2.74)	0.91 (0.03)	8690	1757	79
Pt-14	10	986.3×10^2	27.4	2.52	4.30	50.3 (2.21)	420.6 (0.84)	27.0 (0.96)	150.5 (4.8)	2.23 (0.07)	8690	1275	85.3
Pt-15	12	1051.3×10^2	24.3	2.52	4.30	59.9 (2.63)	470.9 (0.94)	27.3 (0.76)	147.5 (4.4)	3.42 (0.11)	8690	1562	82.0

Table 3. Results of electrolysis of faecal–urine mixture at different potentials
Constant potential electrolysis on platinum at 90 °C

Serial	*Applied potential* /V vs NHE	*Charge* /C	*Electrolysis time* /h	*Initial dry mass of waste* /g		*Gases evolved* /mmol and (g)					*TOC initial* /mg L^{-1}	*TOC final* /mg L^{-1}	*Reduction in TOC* /%
				Faeces solids	*Urine solids*	CO_2	H_2	N_2	O_2	Cl_2			
Pt-10	1.44	15 630	69.83	2.53	4.39	9.5 (0.42)	75.7 (0.15)	11.0 (0.30)	17.0 (0.55)	0.07 (0.001)	8690	6225	28
Pt-7	1.74	28 360	88.30	2.38	4.15	19.0 (0.83)	154 (0.31)	13.0 (0.36)	33.0 (1.05)	0.51 (0.03)	8690	5349	38
Pt-9	1.90	44 030	31.20	2.52	4.32	34.2 (1.50)	202 (0.40)	16.9 (0.47)	43.0 (1.37)	0.82 (0.06)	8690	3501	59
Pt-8RR	2.00	67 300	35.83	2.52	4.30	34.4 (1.51)	256 (0.51)	13.0 (0.36)	78.0 (2.49)	0.87 (0.06)	8690	2959	65

Table 4. Elemental composition in 1 g of artificial faeces mixture

Mass	*Component*	*C* /g	*H* /g	*O* /g	*N* /g	*S* /g	*P* /g	*Salts* /g
0.33 g	Cellulose	0.134	0.018	0.178	–	–	–	
0.20 g	Oleic acid	0.153	0.024	0.023	–	–	–	
0.07 g	*E.coli*	0.035	0.007	0.014	0.007	0.0007	0.0028	
0.35 g	*Torpulina* & Casein	0.112	0.023	0.149	0.065			
0.05 g salt		–	–	–	–	–	–	0.05
1.0 g of faeces mixture contains		0.434	0.072	0.364	0.072	0.0007	0.0028	0.05
Composition of faeces mixture (%)		43.4	7.2	36.4	7.2	0.07	0.28	5

3.2. *Mass balance calculations*

3.2.1. Elemental composition in 1 g of artificial faeces mixture. The assumptions used for the calculations are outlined as follows:

(i) The monomer unit of cellulose was taken to be ($C_6H_{10}O_6$) as given by Chum and Baizer [18].
(ii) The composition of *E. coli* was taken from data of Campbell [19].
(iii) *Torpulina* and Casein were assumed to have the composition of a basic unit of protein (NH_2 CH_2 COOH).

Using the formula weight and the mass fraction of each component in 1 g of the artificial faeces mixture, the elemental composition of the mixture was calculated and is shown in Table 4.

3.2.2. Elemental composition in 1 g of urine solids. The composition of urine varies according to the human diet and health as well as the amount of exercise. The average composition of urine was taken from McGilvery and Goldstein [20]. In these data, an amount equal to 2.8 mol %, is attributed to a number of organic materials depending on the diet and for simplicity this small percentage was assumed to be due to glycine.

The total mass of sodium, potassium, calcium and magnesium salts in the waste mixture was assumed to remain constant during electrolysis and the only function of these salts was to provide conductivity. The NH_4^+ ion was assumed to hydrolyse to ammonia and then undergo oxidation to nitrogen and hydrogen.

Table 5 shows the calculation of the average molecular mass of urine solids and the conversion of the literature values of mole fraction [20] to mass fractions. Using the mass fraction values from Table 5, the elemental composition of urine solids can be presented as shown in Table 6.

The above calculations (Tables 5 and 6) are for 1 g of faeces mixture and 1 g of urine solids, respectively. In this experiment, 2 g of faeces material was dissolved in 140 mL of urine and this quantity of urine contained 3.36 g of urine solids. Thus, weights of C, H, N and O in the experimental mixture were calculated and the weight percentages of the elements are shown in Table 7.

In Figure 7 a flow chart is shown for a run carried out at constant current (Pt 5 in Table 2). The amounts of gases determined by analysis together with the calculated quantities dissolved in water during the collection of gases are indicated in this chart. The amounts of dissolved gases were calculated using Henry's law, the corresponding mole fraction of each gas and the volume of water displaced by the evolved gases. For example, the partial pressure of 53.8 mmol of CO_2 in 617.6 mmol of gas mixture would be 53.8/617.6 atm, i.e., 0.087 atm. The volume of water displaced was 14.52 litres and the solubility of CO_2 at 1 atm and 25 °C is 1.45 g L^{-1}. The amount of CO_2 dissolved is given by $1.45 \times 14.5 \times 0.087$ g, i.e., 1.83 g. By a similar procedure the amounts of other gases dissolved were calculated.

It is seen that out of the 5.36 g of dry solids introduced, 3.4 g have been oxidized. Assuming that the salts introduced with the wastes remain

Table 5. Calculation of the average molecular mass of urine solids and the mass fraction of components therein

	Mole fraction, x	*Molar mass, M*	*Mx*	*Mass fraction*
Na^+	0.200	23	4.60	
K^+	0.055	39	2.15	
Cl^-	0.18	35.5	6.39	0.289 salts
Mg^{2+}	0.007	24.3	0.17	
Ca^{2+}	0.006	40.0	0.24	
NH_4^+	0.036	18	0.648	0.014
Urea	0.454	60	27.24	0.581
Creatinine	0.019	101.0	1.919	0.041
Glucose	0.001	180.0	0.18	0.004
Uric acid	0.003	168.0	0.50	0.010
Glycine	0.037	75.07	2.78	0.059
Net molecular weight of urine solids			46.82	

Table 6. Elemental composition in 1 g of urine solids

Mass fraction	*Component*	*C* /g	*H* /g	*O* /g	*N* /g	*Salts* /g
0.581	Urea	0.116	0.039	0.155	0.273	
0.041	Creatinine	0.015	0.003	0.006	0.017	
0.004	Glucose	0.002		0.002		
0.010	Uric acid	0.003		0.003	0.003	
0.059	Glycine	0.018	0.004	0.025	0.011	
0.015	NH_4^+	–	0.003	–	0.012	
0.288	Salts	–	–	–	–	0.288
1.0 g of urine solids contains		0.154	0.049	0.191	0.316	0.288
Composition of urine solids (%)		15.4	4.9	19.1	31.6	28.8

Table 7. Composition of the experimental faeces–urine mixture

	C /g	*H* /g	*O* /g	*N* /g	*Salts* /g
2.0 g artificial faeces	0.868	0.144	0.724	0.144	0.1
3.36 g solid in 140 ml of urine	0.517	0.165	0.642	1.062	0.97
5.36 g (Total wt of dry mixture)	1.385	0.309	1.366	1.206	1.07
4.29 g (Total wt of dry mixture excluding salts)					
Average wt percent (dry basis) of elements	25.8%	5.8%	25.5%	22.5%	19.9%
Average wt percent (dry basis) of elements excluding salts	32.2%	7.1%	31.8%	28.1%	–

unreacted during the oxidation process, it is now possible to compare the theoretical amounts of CO_2, H_2, O_2 and N_2 with the experimentally determined quantities.

For example, since the percentage of C in the experimental mixture is 32.2% (Table 7), the theoretical amount of carbon dioxide according to the equation $C + O_2 \rightarrow CO_2$ is $3.49 \times 0.322 \times 44/12$, i.e., 4.11 g or 93 mmol. The amounts of other gases expected from the decomposition of the waste were calculated using a similar procedure giving 124 mmol of H_2, 35 mmol of O_2 and 39.3 mmol of N_2. The use of high current densities to achieve higher rates of oxidation of the waste mixture invariably produces simultaneous decomposition of water. The amount of H_2 and O_2 produced by the electrolysis of water is calculated as follows. Mass of water electrolysed is given by mass of gaseous products (8.95 g) *plus* mass of dry solids left after electrolysis (1.87 g) *less* mass of dry solids taken for electrolysis (5.36 g), i.e., 5.46 g. The decomposition of this amount of water produces 303 mmol of H_2 and 152 mmol of O_2. The amount of oxygen consumed to combine with 93 mmol of C to produce CO_2 is 93 mmol.

Thus, the amounts of gases expected on the basis of the above calculations, along with the experimentally

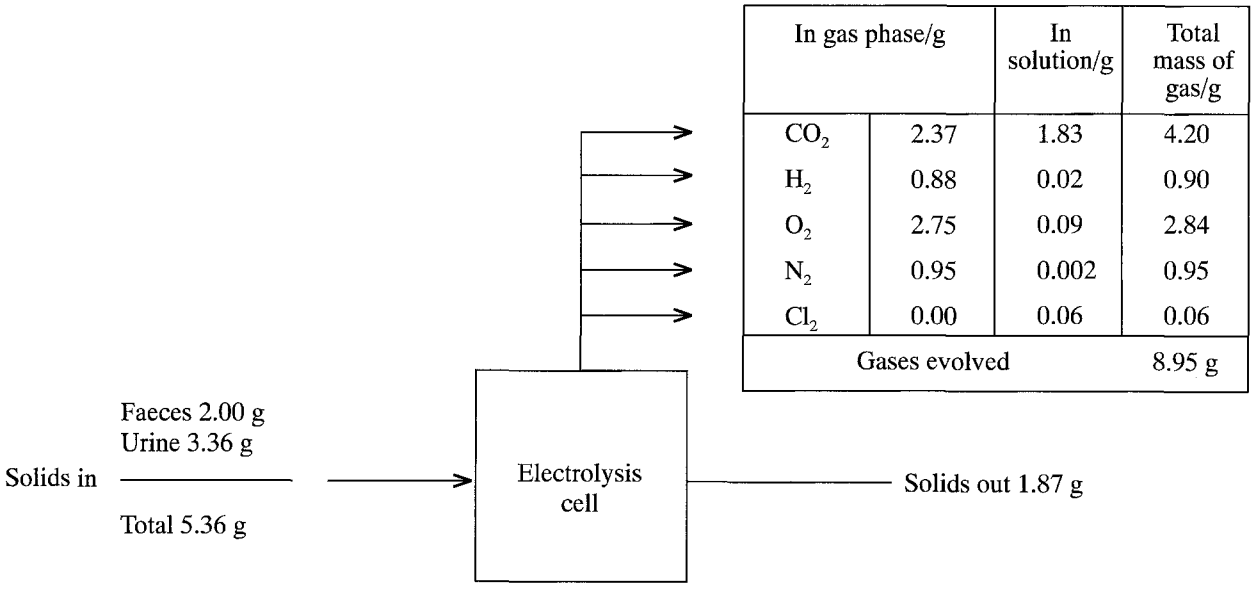

Fig. 7. Flow chart for mass balance calculations using data from experiment Pt-5 in Table 2. Constant current electrolysis in a glass U-tube cell. Current density: 8 mA cm^{-2}, temperature: 90 °C, starting mixture 2 g of artificial faeces mixture in 140 mL of urine. TOC before electrolysis 8690 mg L^{-1}, TOC after electrolysis 1757 mg L^{-1}. Quantity of electricity 105 110 coulombs.

Table 8. Calculated and experimental amounts of gases evolved

Gas	*Calculated* /mmol	*Experimental* /mmol
CO_2	93	95.4
H_2	$(124 + 303^*) = 427$	450
O_2	$[(35 + 152^*) - 93^\dagger$ (for $CO_2)] = 94$	88.8
N_2	39.3	34.0

* Evolved from electrolysis of water.
† Oxygen required for combining with carbon.

obtained values are shown below in Table 8. It is seen from Table 8 that the calculated and experimental values for CO_2, H_2 O_2 and N_2 are in good agreement. Further, the calculated TOC of 9890 mg L^{-1} for the composition of the waste mixture (Table 7) compares well with the experimentally determined value of 9750 mg L^{-1}. Similarly, as the amount of salt in the feed is 1.07 g, the amount of unreacted organic compounds left after electrolysis is 0.80 g; the percentage decomposition is therefore, $(5.36 - 1.07 - 0.8) \times 100/(5.36 - 1.07)$, which is 81% and the measured TOC reduction is 79%. Thus, the elemental compositions of faecal waste and urine assumed in this paper can be used for designing electrochemical reactors for scaling up such a process.

3.3. *Polarization curves obtained using a parallel plate cell*

Figure 8 shows the current-voltage curves obtained with the parallel plate cell for various flow rates at 90 °C. Even using the highest flow rate (512 L h^{-1}), it was only possible to obtain a threefold increase in current density compared with that available at a flat plate without stirring. Thus, it was necessary to investigate the use of other types of electrode configurations for scale up.

3.4. *Parametric studies using a packed bed reactor*

The performance of this three dimensional electrode was assessed by using the space time yield (*STY*) [16] for product formation (CO_2 in this case). This is defined as

$$STY = \frac{\text{Amount of } CO_2 \text{ formed}}{\text{Time} \times \text{cell volume}}$$

This criterion measures the rate of oxidation per unit cell volume.

3.4.1. Dependence of rate of CO_2 generation on bed particle size. Experiments were carried out in the packed bed configuration shown in Fig. 2. The parameters kept constant were bed height (3 cm), current density (7 mA cm^{-2}) based on the area of particles in the bed, and flow rate (550 mL min^{-1}). The variable was the particle size. The average diameters of the particles of Ebonex™ material coated with SnO_2/Sb_2O_3 by the slurry painting method used were 0.35, 0.60, 1.0, 1.85 and 4.0 mm.

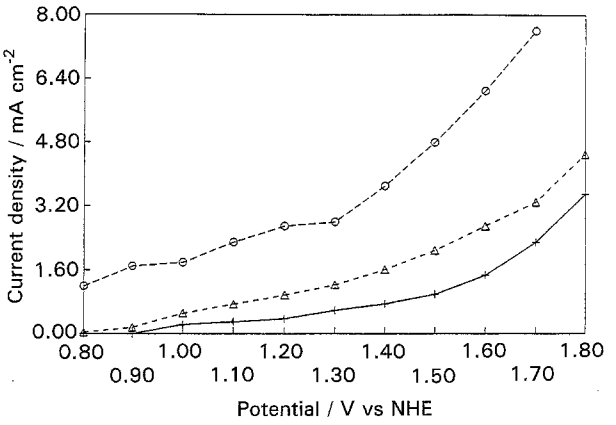

Fig. 8. Hydrodynamic effect on the current density using parallel plate electrochemical cell supplied by Electrocell AB. Waste concentration 14 g of dry waste per litre of urine. Temperature: 90 °C. (+) Without flow: (△) 360 L h^{-1}, (○) 516 L h^{-1}.

The variation of space time yield (*STY*) expressed in mmol of CO_2 h^{-1} cm^{-3} of bed as a function of particle size is shown in Fig. 9.

The rate of generation of CO_2 increases, as expected, as particle size decreases. However, it was found that when the particle size is below 1.0 mm in diameter, variation of the rate of generation reaches a plateau region. As the particle size decreases the area increases and the total current increases. This causes higher rates of gas generation and a decrease of the bed conductivity. Similarly, with small particles, particulate matter may adhere to the particles. This causes contact resistance between particles to increase, making the bed less effective. Thus, the optimal diameter is in the range 0.5 to 1 mm.

3.4.2. Dependence of the rate of CO_2 generation on flow rate. The experiment for this parametric study was carried out using the packed bed configuration shown in Fig. 2. The flow rate varied between 50 and 1275 mL min^{-1} and the other variables, namely particle size (1 mm), current density (4.2 mA cm^{-2}), bed height (5 cm) and temperature (90 °C) were kept constant. The rate of CO_2 production with time was measured by GC.

The variation of *STY* with flow rate is shown in Fig. 10. The rate of generation of CO_2 is independent

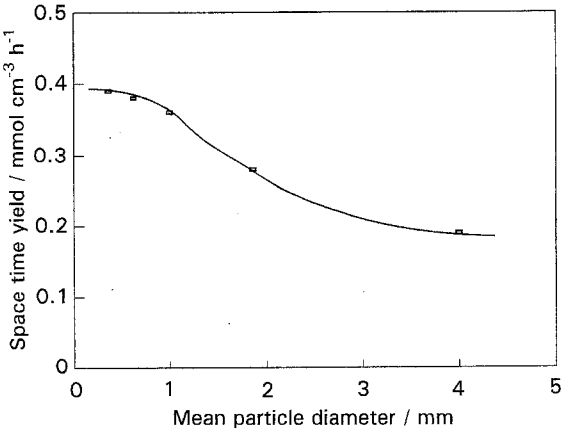

Fig. 9. Variation of space time yield with particle size using the packed bed cell shown in Fig. 2.

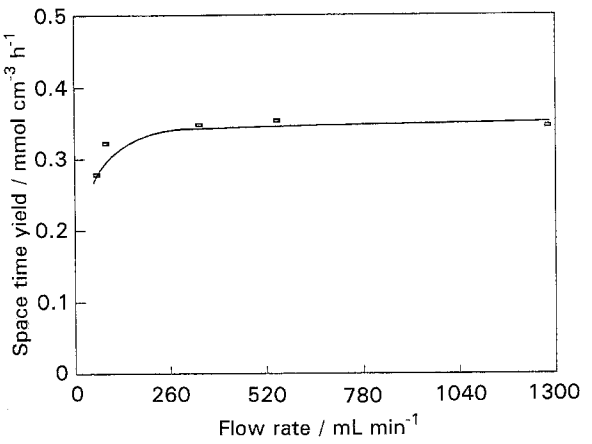

Fig. 10. Variation of space time yield with the flow rate using the packed bed cell shown in Fig. 2.

of flow rate above 350 mL min^{-1}. Similar behaviour was indicated when the parallel plate cell was used. The limiting current increased only by a factor of 3 when the higher flow rate through the cell was used (Fig. 8). To study this effect further, an additional experiment was conducted on a rotating Pt disc electrode. The results are shown in Fig. 11, where the current reaches a plateau at high rotation rates. This confirms that the reaction is kinetically controlled at high rotation speeds.

Thus, it can be concluded that the reaction is not mass transfer controlled above a flow rate of 350 mL min^{-1}. Therefore, a flow rate between 400–600 mL min^{-1} for a bed of cross sectional area of 7 cm^2 is sufficient for the electrochemical reaction to take place in the plateau region, shown in Fig. 10. This corresponds to a linear flow velocity between

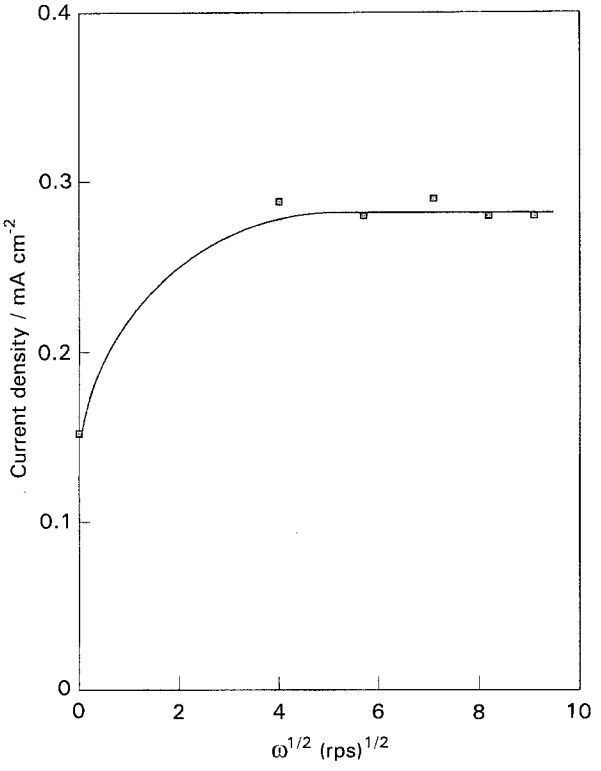

Fig. 11. Variation of current density with the square root of the rotation speed using a platinum rotating disc electrode. Waste concentration 14 g of dry waste per litre of urine. Temperature 90 °C.

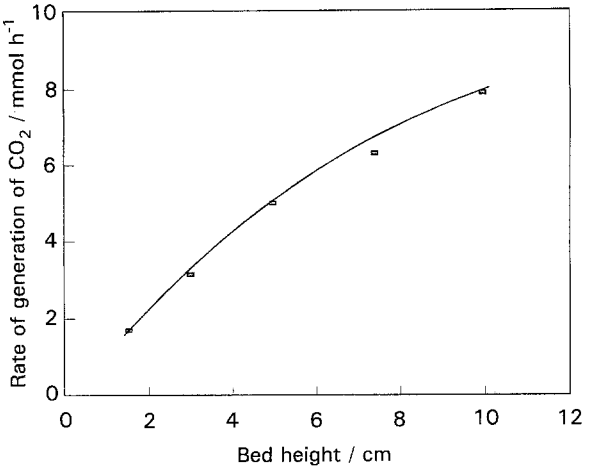

Fig. 12. Rate of generation of carbon dioxide with bed height using the packed cell shown in Fig. 5.

0.9 and 1.4 cm s^{-1} calculated using the cross sectional area of the empty tube. Using a bed voidage, ϵ, of 0.5, the actual velocities within the bed would be in the range 1.8 to 2.8 cm s^{-1}.

3.4.3. Dependence of the rate of generation of carbon dioxide on bed height. The configuration of the packed bed is shown in Fig. 5. The bed height was increased from 1.5 up to 10 cm and at each bed height the generation of carbon dioxide as a function of time was monitored. All other parameters, namely, particle size (1 mm), flow rate (550 mL min^{-1}), current density (4.3 mA cm^{-2}), and temperature (90 °C) were kept constant.

The rate of generation of CO_2 as a function of bed height is shown in Fig. 12. The rate of generation of CO_2 increases with bed height, but Fig. 13 shows that the *STY* decreases with increase in bed height. This indicates that the top part of the bed is not as efficient as the lower part of the bed.

This situation can be explained as follows. The percentage of gas bubbles mixed with the waste mixture increases from the bottom to the top of the bed. Thus, the effective conductivity of the bed gradually decreases. The concentration of reactant also decreases. Both these factors make the upper

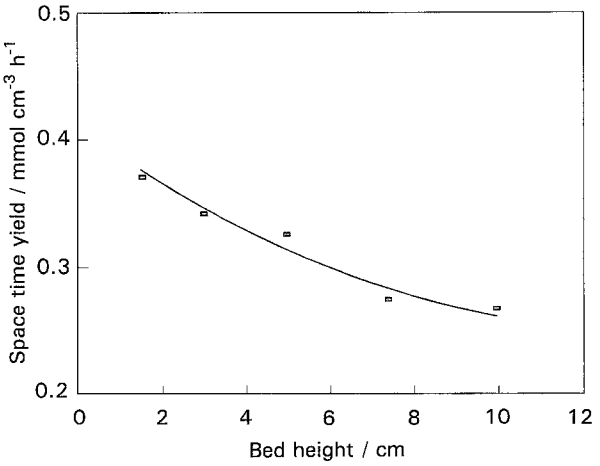

Fig. 13. Variation of space time yield as a function of bed height using the packed bed cell shown in Fig. 5.

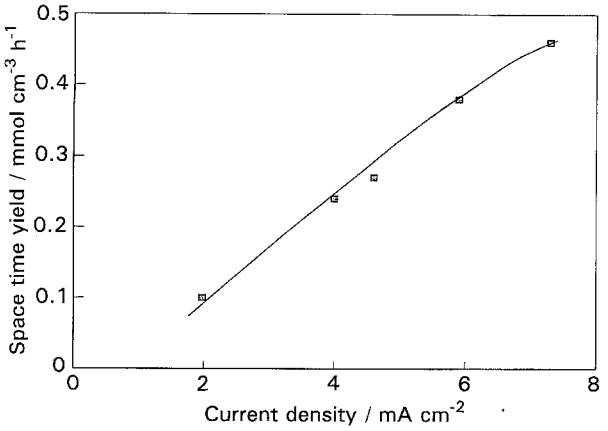

Fig. 14. Effect of current density on the generation of carbon dioxide using the packed bed cell shown in Fig. 5.

part of the bed less effective than the lower part. Thus, it is necessary to limit scale up in the direction flow.

3.4.4. Dependence of the rate of generation of CO_2 on current density. The cell configuration used is shown in Fig. 5. The only variable was the current density. The current density, referred to the surface area of the particles present was increased up to 7.3 mA cm^{-2}. The other parameters, namely, particle size (1 mm), flow rate (550 mL min^{-1}), bed height (9.5 cm), and temperature (90 °C) were kept constant.

The variation of the rate of generation of CO_2 as a function of current is shown in Fig. 14. The rate of generation of CO_2 increases as the current density is increased. However, in practical applications, it is necessary to limit the current density of operation to reduce excessive evolution of oxygen.

The main conclusions of the experiments on the parametric studies are as follows:

(i) The optimal bed particle size is in the range of 0.5 to 1 mm.
(ii) The best flow rate for a bed of 7 cm^2 cross section area is 400–600 mL s^{-1}, which corresponds to a linear flow velocity of 0.9 to 1.4 cm s^{-1}. Higher flow rates do not produce higher oxidation rates, as the reaction is kinetically controlled.
(iii) Increase of bed height increases the conversion of waste to carbon dioxide, but the upper portion of the bed is not as effective as the bottom part of the bed, due to the accumulation of gas bubbles between the particles.
(iv) Increase in current density based on the surface area of particles increases the rate of decomposition of waste at a rate greater than that expected. This is due to the generation of active OH radicals and

Table 9. Elemental composition of average daily waste output of one person on a dry basis

	C	*H*	*O*	*N*	*S*	*P*	*Salts*
Faeces 31.8 g	13.8	2.29	11.58	2.29	0.22	0.089	1.59
Urine 59.0 g	9.1	2.89	11.27	18.64	–	–	16.99
Total 90.8 g	22.9	5.18	22.85	20.93	0.022	0.089	18.58

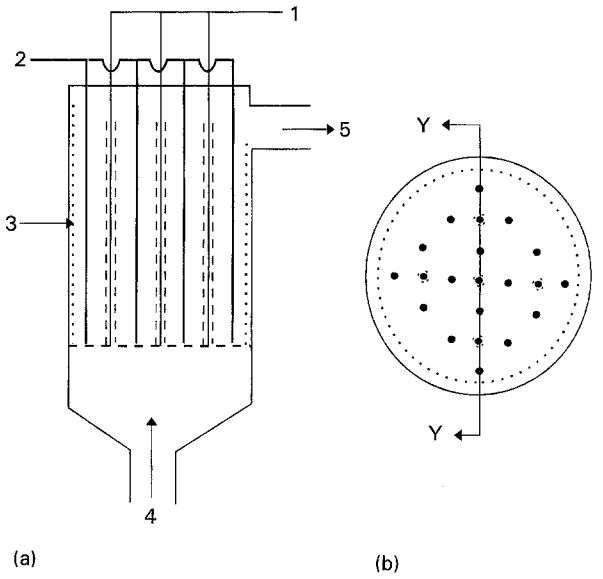

Fig. 15. Design of a cell for breadboard system. (a) Vertical section of cell, (b) horizontal section of cell. (1) Cathode stanchions surrounded by membrane, (2) anode stanchions, (3) current collector mesh, (4) flow inlet and (5) flow outlet.

hypochlorous acid. However, it is necessary to fix the upper limit of the current density to avoid excessive evolution of oxygen.

In summary, particles of Ebonex^{TM} 0.5 mm to 1 mm in diameter coated with SnO_2/Sb_2O_3, a solution flow rate of 0.9 to 1.4 cm s^{-1} through the bed based on the cross sectional area of the empty tube holding the particles, bed heights of 5 to 8 cm, and a current density based on the particle surface area of 5 mA cm^{-2} comprise a suitable set of parameters for the scale up.

A preliminary design of a suitable reactor can now be presented for the electrochemical consumption of human wastes generated by one person per day, in 24 h of electrolysis.

The average daily waste output by one person on a dry basis is 31.8 g of faeces and 59.0 g of urine solids [17]. Using the elemental composition of 1 g of faeces from Table 4 and that of 1 g of urine solids from Table 5, the amount of each element in this daily waste output by one person can be calculated as shown in Table 9.

For preliminary design considerations, the amount of CO_2 expected from the complete conversion of C to CO_2 is calculated as 1900 mmol.

Taking an average value for the *STY* (mmol of CO_2 cm^{-3} h^{-1}) as 0.30*, the volume of the packed bed cell can be calculated:

$$0.30 = \frac{1900}{V \times 24}, \text{ hence, } V = 264\,\text{cm}^3$$

Thus, for a packed bed of height 5 cm, the required diameter would be 8.2 cm.

In this design the cell voltage could be reduced by, say, using five cathode stanchions symmetrically in the

* Although higher values of *STY* up to 0.45 mmol cm^{-3} h^{-1} have been achieved, the value of 0.30 is assumed to take into account any losses in efficiency that might occur due to nonideal fluid flow through the reactor on scale-up.

bed, and four anode stanchions around each cathode stanchion. The cathode stanchions would be insulated from the anode bed particles by Nafion® membranes. A cross section of such a cell is shown in Fig. 15.

4. Conclusions

It is seen that electrochemical oxidation of human waste is feasible and an estimate of the power and energy required to deal with the waste of one person in 24 h can now be calculated.

The total current, ivA, where i is the current density (5 mA cm^{-2}), v is the volume of bed (264 cm^3) and A is the surface area per unit volume of bed (30 cm^{-1}) is $5 \times 264 \times 30$ mA, i.e., 39.7 A. Using a cell voltage of 12 V

$$\text{Power requirement} = 12 \times 39.6 = 475\,\text{W}$$

$$\text{Energy requirement} = \frac{475}{1000} \times 24\,\text{kWh} = 11.4\,\text{kWh}$$

At 5 cents per kWh, the cost of electricity for dealing with one person's waste in 24 h = 57 US cents.

This technology could be appropriate for dealing with human wastes in ships where discharge to sea is no longer permitted.

Acknowledgments

Financial support was provided by NASA Grant NAGW 1779, and also by the trustees of the Welch Foundation in respect to apparatus and equipment. We acknowledge the help from C. E. Verostko of Johnson Space Center, Houston, Texas. We also like to thank N. J. C. Packham of the Lockheed Engineering and Sciences Company and R. Sundaresan for helpful discussions.

References

[1] G. T Miller, 'Environmental Science; Sustaining the Earth', Wordsworth Publishing Company, Belmont, CA, 4th edn. (1992) p. 253.
[2] M. Holtzapple and F. Little, 'Regenerative Life Support System', Research and Concept Program Report, Dec. (1988), NASA NAJ-253.
[3] W. Strauss, in 'Environmental Chemistry', (edited by J. O'M. Bockris), Plenum Press, New York (1977) p. 179.
[4] D. J. Spedding, *in ibid.*, p. 213.
[5] J. O'M. Bockris, B. J. Piersma and E. Gileadi, *Electrochim. Acta* **9** (1964) 1329.
[6] P. M. Dhooge, J. Space Manufacturing. Proceedings of the 8th Princeton/AIAA/SSI Conference, American Institute of Aeronautics and Astronautics, Washington, DC (1987).
[7] R. C. Tischer, L. R. Brown and M. V. Kennedy, *Dev. Ind. Microbiol.* **6** (1965) 238.
[8] L. Kaba, G. D. Hitchens and J. O'M. Bockris, SAE Technical Paper Series, 891510, 19th Intersociety Conference on Environmental System, San Diego, CA, July (1989).
[9] L. Kaba, G. D. Hitchens and J. O'M. Bockris, *J. Electrochem. Soc.* **137** (1990) 1341.
[10] R. C. Bhardwaj, D. K. Sharma and J. O'M. Bockris, Report to NASA on Grant NAGW 1779, Aug. (1990).
[11] R. Kotz, S. Stucki and B. Carcer, *J. Appl. Electrochem.* **21** (1991) 14.
[12] S. Stucki, R. Kotz, B. Carcer and W. Suter, *ibid.* **21** (1991), 99.
[13] Ch. Comnisellis and G. P. Vercesi, *ibid*, **21** (1991) 136.
[14] A. C. Guyton, 'Textbook of Medical Physiology', 6th edn, McGraw-Hill, New York (1981).
[15] Ch. Comnisellis and C. Pulgarin, *J. Appl. Electrochem.* **23** (1993) 108.
[16] D. Pletcher, 'Industrial Electrochemistry', Chapman & Hall, London (1982) p. 60.
[17] C. E. Verotsko (NASA Johnson Space Center), Private communication.
[18] H. L. Chum and M. M. Baizer, 'The Electrochemistry of Biomass and Derived Materials'. ACS Monograph 183, American Chemical Society (1985) p. 85.
[19] N. A. Campbell, 'Biology', Benjamin–Cummings Publishers, Redwood City, CA, 2nd edn (1990).
[20] R. W. McGilvery and A. W. Goldstein, 'Biochemistry: A Functional Approach', Saunders Company, 3rd edn, p. 754.